Zeitschrift: Schweizerische mineralogische und petrographische Mitteilungen = Bulletin suisse de minéralogie et pétrographie

Band: 78 (1998)

Heft: 1

Artikel: Polyphase structural, intrusive and metamorphic evolution of the Bockfjorden area, NW Spitsbergen

Autor: Wyss, Martin / Hermann, Jörg / Müntener, Othmar

DOI: https://doi.org/10.5169/seals-59276

Nutzungsbedingungen

Die ETH-Bibliothek ist die Anbieterin der digitalisierten Zeitschriften auf E-Periodica. Sie besitzt keine Urheberrechte an den Zeitschriften und ist nicht verantwortlich für deren Inhalte. Die Rechte liegen in der Regel bei den Herausgebern beziehungsweise den externen Rechteinhabern. Das Veröffentlichen von Bildern in Print- und Online-Publikationen sowie auf Social Media-Kanälen oder Webseiten ist nur mit vorheriger Genehmigung der Rechteinhaber erlaubt. Mehr erfahren

Conditions d'utilisation

L'ETH Library est le fournisseur des revues numérisées. Elle ne détient aucun droit d'auteur sur les revues et n'est pas responsable de leur contenu. En règle générale, les droits sont détenus par les éditeurs ou les détenteurs de droits externes. La reproduction d'images dans des publications imprimées ou en ligne ainsi que sur des canaux de médias sociaux ou des sites web n'est autorisée qu'avec l'accord préalable des détenteurs des droits. En savoir plus

Terms of use

The ETH Library is the provider of the digitised journals. It does not own any copyrights to the journals and is not responsible for their content. The rights usually lie with the publishers or the external rights holders. Publishing images in print and online publications, as well as on social media channels or websites, is only permitted with the prior consent of the rights holders. Find out more

Download PDF: 30.04.2026

ETH-Bibliothek Zürich, E-Periodica, https://www.e-periodica.ch

SCHWEIZ. MINERAL. PETROGR. MITT. 78, 87–106, 1998

Polyphase structural, intrusive and metamorphic evolution of the Bockfjorden area, NW Spitsbergen

by *Martin Wyss*[1,2], *Jörg Hermann*[1], *Othmar Müntener*[1] and *Liane Benning*[1,3]

Abstract

Structures, intrusive contacts and metamorphic mineral assemblages reveal a polyphase tectonothermal evolution for the Caledonian basement rocks of the Bockfjorden area, NW Spitsbergen. The oldest deformation D_1 is documented by isoclinal folds F_1 in biotite schist. F_1 folds are crosscut by an intrusion I_1 of tonalitic to monzogranitic composition. Both, F_1 folds and I_1 are overprinted by D_2 structures, that are considered to be related to the Silurian Caledonian continental collision. D_1 and I_1 are thus regarded as the record of a complex pre-Silurian evolution of the basement rocks. The Caledonian continental collision that is represented by the isoclinal folding F_2 and by the main schistosity S_2 was simple shear dominated and associated to S–N thrusting in the studied area. During D_2 the I_1 granitoid rocks were transformed to orthogneiss. The related metamorphism M_2 reached upper amphibolite facies conditions. During or after late stage D_2 deformation the orthogneiss provides evidence for incipient partial melting. The resulting migmatites and S_2 were subsequently crosscut by the granodiorite and monzogranite of the intrusive event I_2, that display partly a peraluminous composition, pointing to partial melting of crustal rocks as the magma source. Subsequently, cordierite formed in all Al-rich rock types including I_1 and I_2 rocks. Cordierite growth was caused by a high T–low P metamorphism at conditions of 630–700 °C and 0.3–0.4 GPa, the geotherm of which was about 50°/km. The transition from migmatite formation to granite emplacement followed by a high T–low P metamorphism indicates near isothermal decompression under upper amphibolite facies conditions. This evolution reflects a continuous exhumation of mid-crustal rocks that is considered as the consequence of crustal extension during the collapse of Caledonian thickened crust.

Keywords: metamorphic rocks, structural geology, tectonothermal evolution, Caledonian basement, NW Spitsbergen.

Introduction

The Caledonian convergence in Spitsbergen can be subdivided into a Middle Ordovician subduction and a later Middle Silurian continental collision (OHTA et al., 1984; DALLMEYER et al., 1990). Evidence for subduction is given by eclogites and blueschists integrated in the pre-Devonian basement rocks. However, most of the features recorded in the basement rocks were caused by continental collision including several generations of deformation, high grade metamorphism, formation of migmatites and intrusion of syn- and post-tectonic granites (HJELLE, 1979; HJELLE and LAURITZEN, 1982). Recent age determinations indicate that magmatism within the pre-Devonian basement is not restricted to the Late Caledonian (PEUCAT et al., 1989; GEE et al., 1992; GEE et al., 1994; OHTA, 1992; OHTA, 1994). This provides evidence for a long and complex history of the basement rocks.

In this study a detailed investigation of the pre-Devonian basement rocks in the Friedrichbreen area in Bockfjorden, NW Spitsbergen is presented. The first part comprises a geological map and detailed petrographic descriptions of the rock types. In the second part new bulk- and trace element data of the intrusive rocks are presented and in the third part we describe intrusive relationships, overprinting structures and metamor-

[1] Institut für Mineralogie und Petrographie, ETH Zentrum, CH-8092 Zürich, Switzerland.
[2] Present address: Institut de Minéralogie et Pétrographie, Université de Lausanne, BFSH2, CH-1015 Lausanne, Switzerland. (corresponding author)
[3] Present address: Pennsylvania State University, Department of Geosciences, University Park, PA 16802 USA.

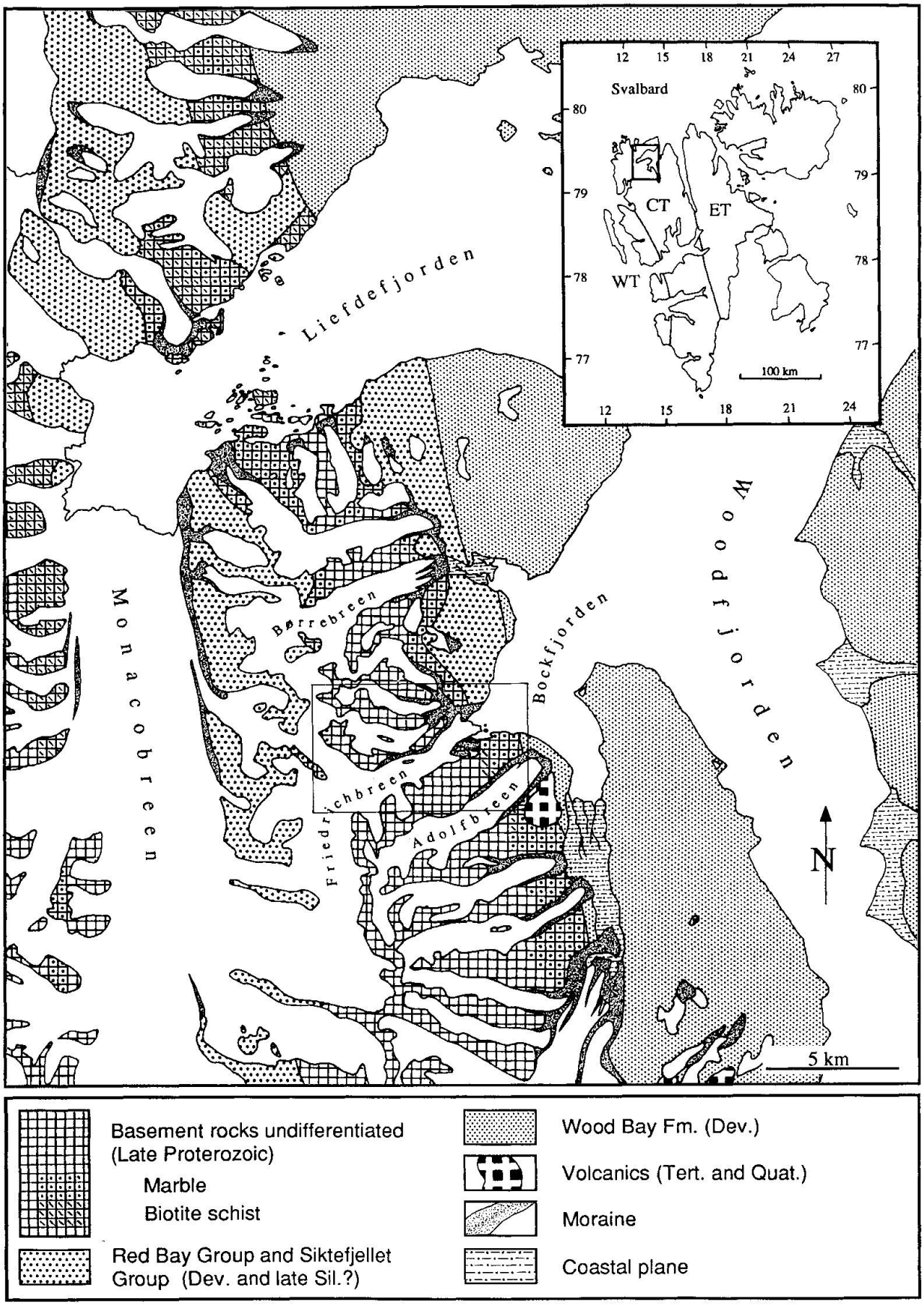

Fig. 1 Map of the Woodfjorden-Liefdefjorden region, Northwestern Spitsbergen, Svalbard. Inset: Subdivision of Svalbard in three terranes: WT = Western Terrane, CT = Central Terrane, ET = Eastern Terrane. Frame: geological map of the Smørstabben-Friedrichbreen-Krona region, figure 2.

phism, on the basis of which we subdivide the complex evolution of the pre-Devonian basement rocks into distinct events. Particular emphasis will be placed on the first deformation D_1 and the first magmatic event I_1 predating the Silurian collision. We will also underline the subdivision of the late Caledonian orogeny into four tectonothermal events, that allow a detailed reconstruction of the thermal history postdating crustal thickening. Finally, the significance of simple shear dominated structures will be discussed in relation to continental collision.

Geological setting

The metamorphic rocks examined in the present investigation are part of the basement ridge between Woodfjorden and the northern part of the Monacobreen (Fig. 1). HOLTEDAHL (1914) was the first to mention these rocks as Hecla Hoek rocks in this area. Later, GEE and MOODY-STUART (1966), GJELSVIK (1979), HJELLE and LAURITZEN (1982) and PIEPJOHN et al. (1992) described the so called lower Hecla Hoek rocks in detail. HARLAND and WRIGHT (1979) subdivided the pre Devonian basement of Svalbard into three terranes (Fig. 1), the Bockfjorden area belonging to the Central Terrane. According to GJELSVIK (1979), the lower Hecla Hoek succession is mainly composed of metamorphic carbonates and pelites, as well as of various amounts of granite, gneiss and migmatites. In the present investigation, the metasediments and essentially the granites, gneiss and migmatites are described in detail. Quarternary volcanism in the Bockfjorden region occurred along Devonian faults and has been described in detail by AMUNDSEN (1987) and by TUCHSCHMID and SPILLMANN (1992).

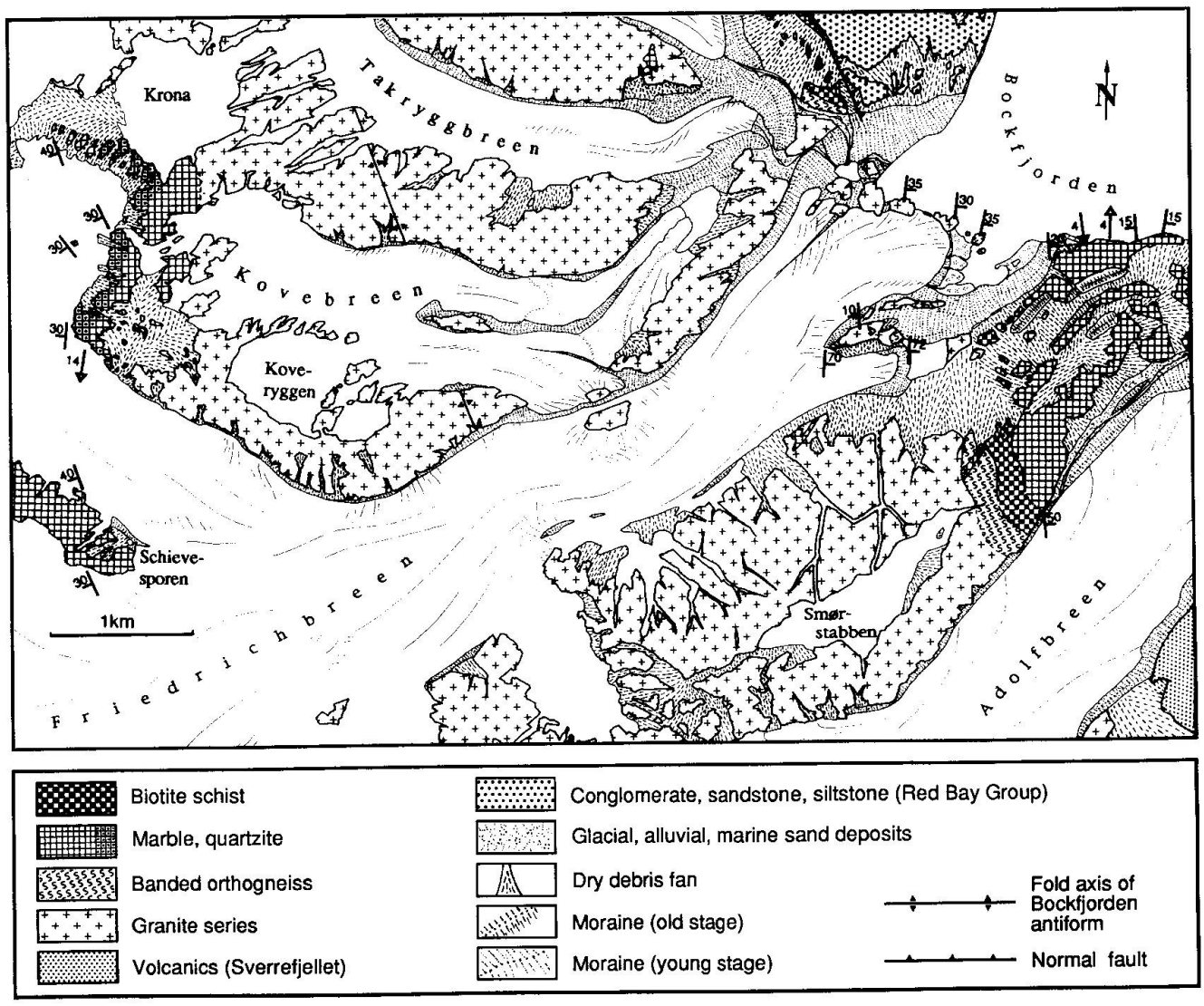

Fig. 2 Geological map of the Smørstabben-Friedrichbreen-Krona region. Arrows: stretching lineations with dip angle indicated; dip-symbols: strike and dip of B_0 and S_2 with dip angle indicated.

Tab. 1 Mineral assemblages related to the different metamorphic and igneous stages discussed in the text. Ab = albite, Bt = biotite, Cal = calcite, Chl = chlorite, Crd = cordierite, Di = diopside, Ep = epidote, Grt = Garnet, Hbl = hornblende, Hu = humite-minerals, Kfs = K-feldspar, Ms = muscovite, Ol = olivine, Phl = phlogopite, Pl = plagioclase, Qtz = quartz, Scp = scapolite, Sil = sillimanite, Spl = spinel, Tr = tremolite, Ves = vesuvianite, Wo = wollastonite, Wm = white mica.

	biotite schist	**marble**	**banded orthogneiss**	**granodiorite**	**monzogranite and schlieren granite**
D_1 deformation	Bt				
I_1: First phase of magmatism			Qtz + Kfs + Pl + Bt ± Grt (?) [a]		
D_2 deformation M_2 metamorphism	Bt + Sil + Qtz	Di + Phl	Bt + Sil + Qtz ± Grt		
I_2: second phase of magmatism		[b]		Qtz + Pl + Kfs + Bt ± Grt (?) [a]	Qtz + Pl + Kfs + Bt [a]
High T–low P metamorphism	Bt + Kfs + Pl + Qtz + Crd ± Sil [c]	Cal + Qtz + Pl + Scp + Di + Phl Ol + Spl + Cal ± Chl ± Hbl	Bt + Kfs + Pl + Qtz + Crd ± Sil [d]	Bt + Kfs + Pl + Qtz + Crd ± Sil [d] ± Grt [d]	Qtz + Pl + Kfs + Bt
Retrograde metamorphism [e]	Chl + Wm + Ab + Qtz	Tr + Chl + Cal ± Dol	Chl + Wm + Ab + Qtz	Chl + Wm + Ab + Qtz	

[a] assumed magmatic paragenesis based on norm calculations
[b] parageneses developed during contact metamorphism: Cal + Qtz + Wo + Di; Grt + Ves + Ep + Chl; Di + Qtz + Kfs + Cal; Phl + Hu +Di + Cal
[c] in more mafic layers: pyroxene + amphibole
[d] as inclusions in plagioclase and cordierite
[e] pinitization and formation of myrmekites in all rock types (except in the marbles)

Petrography

In the investigated area rocks of the pre-Devonian basement have been mapped. The basement rocks are subdivided into metasediments, the banded orthogneiss and the granite series, from oldest to youngest (Figs 2, 3).

The metamorphic mineral assemblages that occur in these rock types are summarized in table 1.

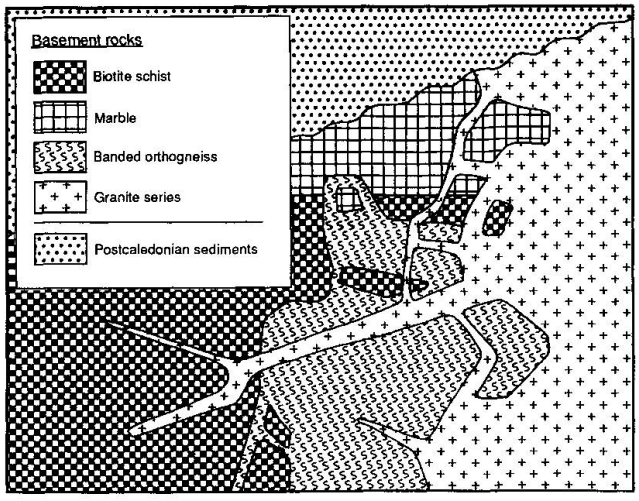

Fig. 3 Stratigraphic relationships of the lithologies in the Bockfjorden area; not to scale.

METASEDIMENTS

Biotite schist

The biotite schist occurs in the eastern part of the studied area with a maximal thickness of about 100 meters (Fig. 2). It is characterized by a compositional banding of most probably sedimentary origin. Occasionally, it is interlayered with gneiss and/or quartzite and crosscut by discordant pegmatites.

The biotite schist is composed of various amounts of porphyroblastic biotite, quartz, K-feldspar and plagioclase. It also contains cordierite, relic garnet and rare sillimanite, the occurrence of which is bound to distinct layers, depending on the primary sedimentary composition of the rocks. Locally, clinopyroxene, hornblende and titanite are observed. Retrograde crystallization includes pinitization of cordierite, crystallization of white mica, transformation of biotite to chlorite and myrmekite growth in K-feldspar.

Marbles and associated rocks

Most of the carbonate rocks encountered in the area are impure, coarse-grained, grey-yellow calcite marbles. The most characteristic feature of

these rocks are intercalated, intensely folded and/or boudinaged sedimentary layers of metapelitic to metabasic composition. At the western slope of Koveryggen (Fig. 2), huge lenses of fine-grained quarzite are interbedded with the marble. In general, two different types of marbles are distinguished:

1) A silica saturated calcite marble containing the mineral assemblage calcite + diopside + plagioclase + scapolite + phlogopite + quartz. Accessories are apatite, titanite, hematite and magnetite.

2) A silica undersaturated marble with olivine + spinel + chlorite + calcite + dolomite ± humite minerals ± pargasitic amphibole ± phlogopite.

The metapelitic to metabasic layers contain various amounts of biotite, hornblende, white mica, rutile and rarely sillimanite. The quartzite contains biotite and sillimanite. Minor amounts of plagioclase and K-feldspar as well as accessory tourmaline and apatite occur.

Retrograde crystallization of tremolite + calcite + chlorite is widespread. In the silica undersaturated marble tremolite and dolomite grew at the expense of olivine + calcite. Locally, retrograde Mg-chlorite and serpentine overgrew spinel and olivine, respectively.

At the eastern slope of Schievesporen (Fig. 2), the high-grade marble is overprinted by an intense mylonitic foliation. This led to grain size reduction and to a retrograde crystallization of tremolite + calcite ± dolomite ± white mica ± serpentine.

Marble xenoliths within the intrusive rocks north of Takryggbreen display different mineral assemblages (Tab. 1). They are up to several tens of meters thick and display coarse-grained (up to 1 cm) polygonal textures.

BANDED ORTHOGNEISS (INTRUSIVE EVENT I_1)

The occurrence of the grey to dark grey banded orthogneiss is limited to narrow zones between the metasediments (biotite schist and marbles/quartzite) and the granodiorite (granite series) in the eastern part and between the metasediments and the monzogranite (granite series) in the western part, respectively (Fig. 2). It is partly discordant towards the biotite schist and towards the marbles and it is crosscut by the granodiorite and monzogranite of the granite series. The banded orthogneiss is characterized by a strong schistosity and by a compositional banding, consisting of leucocratic and melanocratic layers (Fig. 4a). Both, biotite schist and marbles/quartzite appear as xenoliths in the banded orthogneiss. Cm- to dm-scale quartz nodules contain occasionally prismatic andalusite intergrown with acicular sillimanite/fibrolite.

The normative magmatic mineral assemblage ranges between monzogranitic and tonalitic compositions. Melanocratic layers contain biotite, oligoclase, cordierite and minor quartz and K-feldspar. Leucocratic layers are characterized by abundant quartz, K-feldspar and cordierite with minor biotite. Biotite is partly intergrown with acicular sillimanite. Staurolite and garnet are restricted to a few samples from melanocratic layers. K-feldspar grains contain rounded quartz- and biotite inclusions; occasionally, they show transformation to myrmekites along grain boundaries. Cordierite generally displays inclusions of rounded quartz and biotite (Fig. 4b) and of acicular sillimanite (Fig. 4c). Oligoclase displays inclusions of acicular sillimanite, too (Fig. 4c). Retrograde alteration of the previous minerals includes pinitization, chloritization and/or coarse muscovite overgrowth on cordierite (Fig. 4b), saussuritization of plagioclase and replacement of biotite by chlorite.

GRANITE SERIES (INTRUSIVE EVENT I_2)

In the granite series, rocks of granodioritic and of monzogranitic composition can be distinguished. The monzogranites are subdivided into monzogranites ss. and monzogranitic schlieren granites. Sharp, mappable boundaries between these rock types do not exist in the Bockfjorden area except for dikes.

Granodiorite

The granodiorite occurs as a large intrusive body which includes xenoliths of banded orthogneiss and of metasediments. Rare dikes of granodiorite crosscut the country rocks. Xenoliths of fine-grained massive biotite fels have been found. The contact to the banded orthogneiss is either sharp or diffuse.

The granodiorite is light grey to grey and generally homogeneous. Towards its borders it is weakly foliated. Locally, nearly round, cm- to dm-scale quartz-feldspar nodules occur.

The normative magmatic mineral assemblage ranges between granitic and granodioritic compositions. Main metamorphic minerals are quartz, plagioclase, cordierite, K-feldspar and biotite. Plagioclase is often zoned (An_{15-30}) and contains rare inclusions of acicular sillimanite and/or garnet.

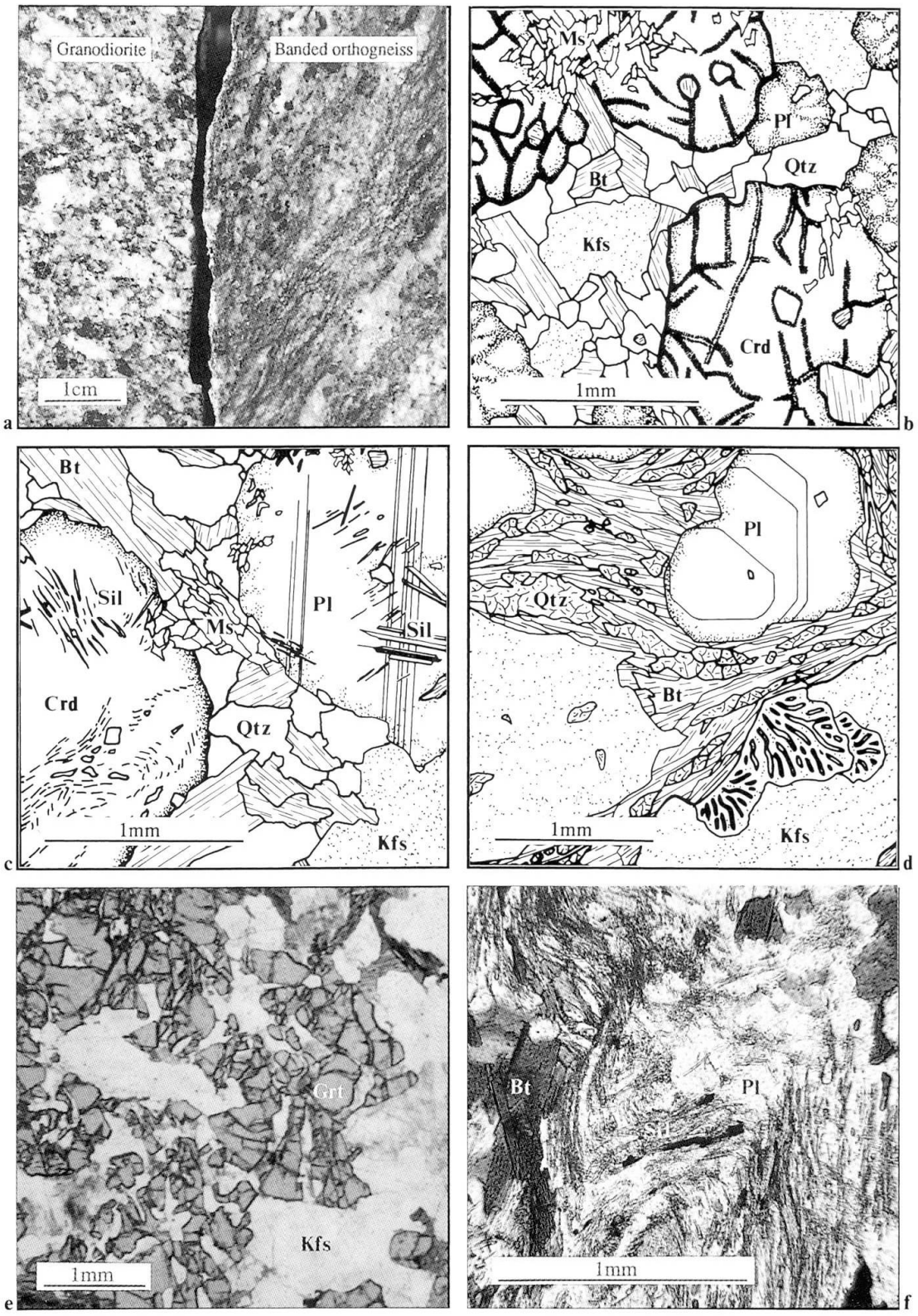

Fig. 4 *(a)* Polished hand specimens of granodiorite (left) and of banded orthogneiss (right). Most of the dark grains are cordierite. *(b)* Banded orthogneiss: cordierite is marginally pinitized and displays rounded inclusions of quartz and biotite (drawing after photomicrograph). *(c)* Banded orthogneiss: cordierite and plagioclase contain inclusions of acicular sillimanite (drawing after photomicrograph). *(d)* Monzogranite: K-feldspar displays myrmekites, plagioclase is slightly zoned (drawing after photomicrograph). *(e)* Garnet-bearing aplite: poikiloblastic garnet (photomicrograph). *(f)* Xenolith of biotite schist: inclusions of F_3-folded acicular sillimanite in plagioclase (photomicrograph). Abbreviations are: Bt = biotite, Crd = cordierite; Kfs = K-feldspar; Ms = muscovite, Pl = plagioclase; Qtz = quartz; Sil = sillimanite.

Cordierite crystals contain rounded inclusions of quartz and biotite as well as acicular sillimanite and/or rare garnet. Retrograde chloritization and pinitization vary strongly in intensity. K-feldspar commonly displays myrmekite growth and retrogression to muscovite along grain boundaries. In some samples, biotite is intergrown with rutile and/or altered to chlorite.

Monzogranite

The monzogranite is characterized by a dark grey color and a granoblastic texture. It mainly occurs on Koveryggen (Fig. 2), where it is in direct contact with metasediments. It contains xenoliths of orthogneiss and of metasediments.

The monzogranite consists of porphyroblasts of K-feldspar and oligoclase which are surrounded by a very fine-grained matrix of quartz, plagioclase, K-feldspar and biotite (Fig. 4d). Sometimes, plagioclase exhibits a magmatic zonation, ranging from andesine cores to oligoclase rims. Occasionally, plagioclase contains inclusions of sillimanite fibres. Retrograde crystallization includes myrmekite growth on the grain boundaries of K-feldspar (Fig. 4d), saussuritization of plagioclase and the development of quartz subgrains.

Schlieren granite

This granite crops out on Koveryggen. It has never been found in contact to metasediments. The schlieren granite is always massive and of a light grey color. It is characterized by nebulous inhomogeneities of magmatic origin caused by differences in mineral ratios (BATES and JACKSON, 1987).

The medium-grained schlieren granite is of monzogranitic composition, consisting of K-feldspar, oligoclase, quartz and biotite. K-feldspar as well as oligoclase show rounded inclusions of quartz. Some plagioclase is slightly zoned. Myrmekite growth along the grain boundaries of K-feldspar and subgrain formation in quartz are common.

Dikes

The dikes are mostly observed inside the granite series, they rarely occur outside. No contact phenomena in the surrounding rocks such as contact-metamorphosed or metasomatized rims have been observed. Aplites and pegmatites are of a planar shape, the garnet-bearing aplites are mostly of an irregular shape.

Aplites: The aplites are undeformed and sharply crosscut the granodiorite. Their normative mineral assemblage is of syenogranitic composition. Main metamorphic components are fine-grained K-feldspar, quartz, plagioclase, rare cordierite and biotite. K-feldspar and plagioclase crystals are interspersed with rounded quartz inclusions, K-feldspar displays myrmekite formation at the grain boundaries and plagioclase shows strong sericitization. Cordierite is often pinitized and/or overgrown by chlorite. Biotite is generally altered to chlorite.

Garnet-bearing aplites: The garnet-bearing aplites are of a very irregular shape and crosscut the granodiorite and the monzogranite (Fig. 5, loc. 1 and 2). Their contacts to the granodiorite and monzogranite can be both sharp or indistinct.

The syenogranitic, medium-grained mineral assemblage consists of K-feldspar, quartz, plagioclase, biotite and some poikilitic garnet of up to 1 cm in diameter (Fig. 4e). Some plagioclases are slightly zoned, biotite occasionally displays inclusions of sillimanite. Retrograde crystallization includes alteration of biotite to chlorite and the decomposition of garnet to biotite, plagioclase, hematite and chlorite along cracks. Allanite is a rare accessory mineral.

Pegmatites: Pegmatites contain variable amounts of plagioclase, K-feldspar, quartz and often diopside. K-feldspar is commonly overgrown by myrmekite, plagioclase is saussuritized and diopside is converted to green hornblende and biotite. Calcite is a frequent accessory mineral.

CORRELATION OF ROCK TYPES

The association of rock types in the Bockfjorden area is similar to the one reported from the lower Hecla Hoek of NW Spitsbergen east of Monacobreen (GEE and HJELLE, 1966; HJELLE, 1979; GJELSVIK, 1979). The granite series may correspond to the late tectonic grey granitic rocks of HJELLE (1979), that are closely associated with layered gneisses and migmatites (HJELLE and OHTA, 1974; HJELLE, 1979). These layered gneisses and migmatites partly show the same features as the banded orthogneiss in the studied area.

GEE and HJELLE (1966) defined the Generalfjella Formation in which marbles are widespread. It has been suggested that the marbles in the Bockfjorden area also belong to this formation (GJELSVIK, 1979). However, there is an uncertainty in this correlation as it is not clear if both rock associations underwent a similar structural evolution and as no detailed age determinations exist.

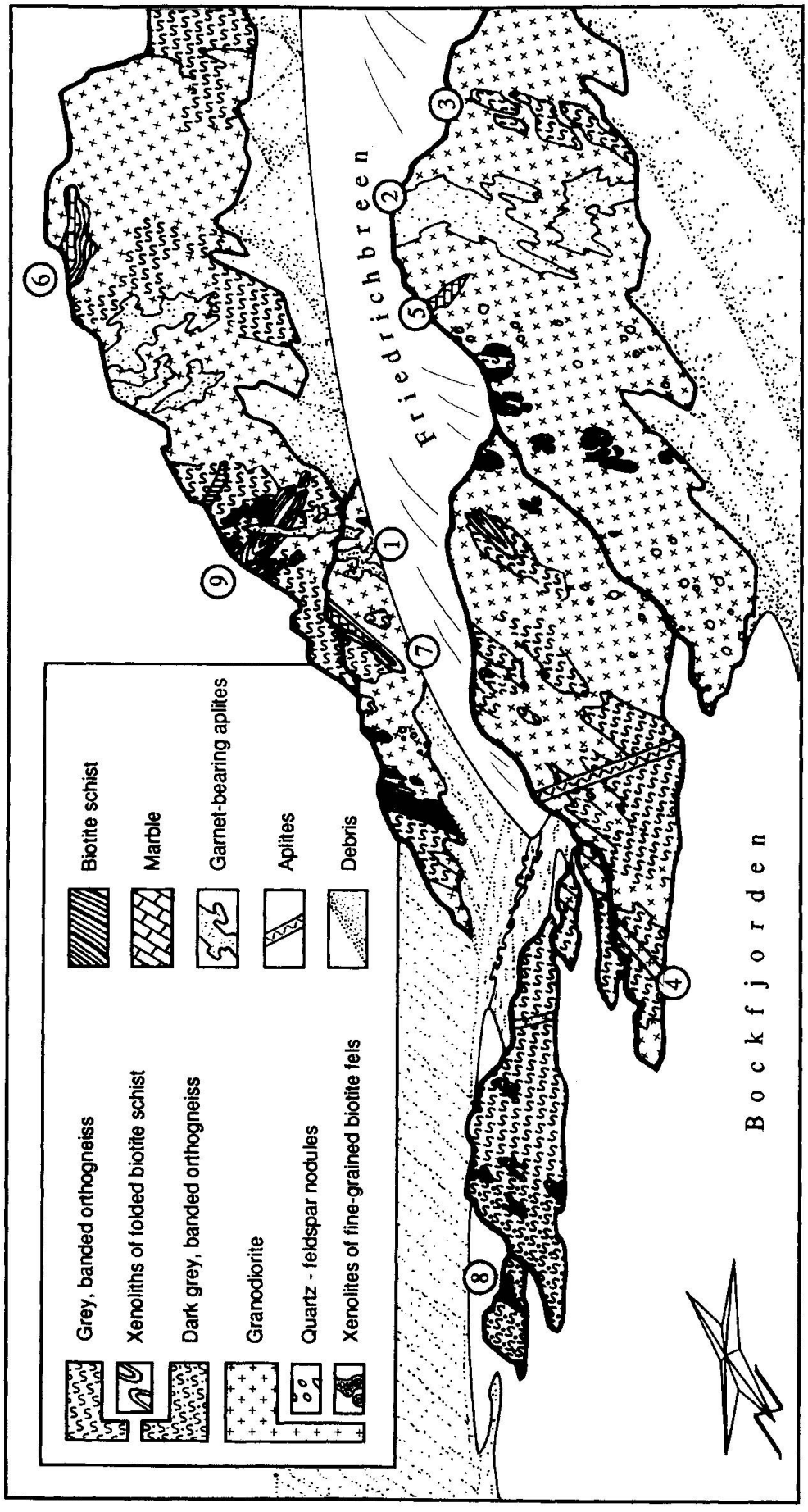

Fig. 5 Intrusive relationships at the eastern border of the granite series, below the glacier tongue of Friedrichbreen. Explanations to localities 1–9 are given in the text. View from north to south. Scale: locality 5: 1 cm = 1.5 m; locality 9: 1 cm = 20 m.

In addition, the thickness of these rock types is quite different. GEE and HJELLE (1966) reported 2000 metres of Generalfjella formation sediments, whereas the biotite schist and marble in the Bockfjorden area have a maximum thickness of about 600 metres.

Bulk rock chemistry of the intrusive rocks

In the investigated area two intrusive events are distinguished: an older intrusion I_1 of tonalitic to monzogranitic composition and the younger granite series (intrusion I_2). The intrusion I_1 is completely transformed to banded orthogneiss by the deformation D_2. The younger granite series I_2 by contrast crosscut the D_2 structures. Xenoliths of banded orthogneiss are widespread within the granite series. The intrusive contacts are best exposed in front of the glacier tongue of Friedrichbreen (Fig. 2). A detailed overview of this area is given in figure 5, showing the field relationships between the observed rock types.

Bulk rock analyses of biotite schist, of banded orthogneiss and of different rock types of the granite series (Tab. 2) were carried out in order to clarify four problems:

1) *Is there a difference in the chemical composition of the rocks belonging to the two magmatic events I_1 and I_2?* The major elements show similar distribution patterns for I_1 and I_2 rocks, an example of which is given in figure 6. The distribution patterns of minor- and trace elements are very similar for the I_1 rocks (pattern 3; Fig. 7 and Tab. 3) and for part of the I_2 rocks (granodiorite, pattern 1; Fig. 7 and Tab. 3). Another part of the I_2 rocks (monzogranite, schlieren granite, garnet-bearing aplite and sample B11 of granodiorite) is characterized by pattern 2 (Fig. 7 and Tab. 3). Therefore, neither major element- nor minor- and trace element distribution patterns provide arguments for a clear chemical distinction of the rocks of the two magmatic events I_1 and I_2.

2) *Do the magmas of I_1 and I_2 represent partial melts of the upper mantle or do they represent partial melting of the crust?* In the rocks of I_1 as well as in the rocks of I_2 the K_2O, FeO_{tot}, Al_2O_3 and SiO_2 content varies strongly (Tab. 2). However, the $MgO/MgO + FeO_{tot}$-ratio remains almost constant (Fig. 6). This demonstrates, that the melts of I_1 and I_2 did not undergo large fractionation during their intrusion. By contrast, in differentiated intrusions the mafic index decreases with increasing SiO_2-content. Therefore, the magmas of I_1 and I_2 do not represent differentiated melts from an upper mantle source. This is supported by the lack of mafic enclaves that crystallized from more primitive melts in differentiated intrusions (CHAPPELL and WHITE, 1974). The mostly peraluminous chemistry (Tabs 2, 3) of the granite series and of the orthogneiss classifies these rocks as

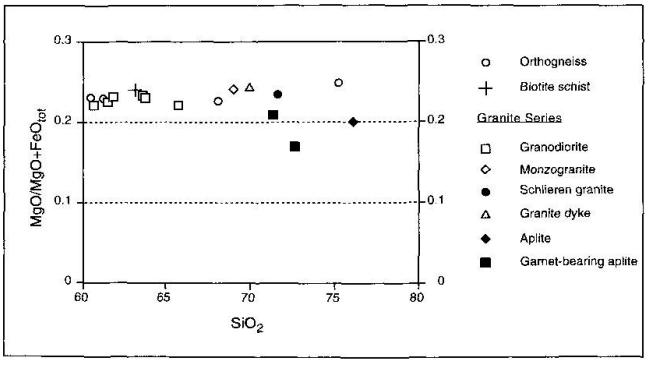

Fig. 6 Major elements plotted in a SiO_2 versus $MgO/MgO + FeO_{tot}$ diagram. The distribution pattern is representative for K_2O-, FeO_{tot}- and Al_2O_3 versus $MgO/MgO + FeO_{tot}$ diagrams.

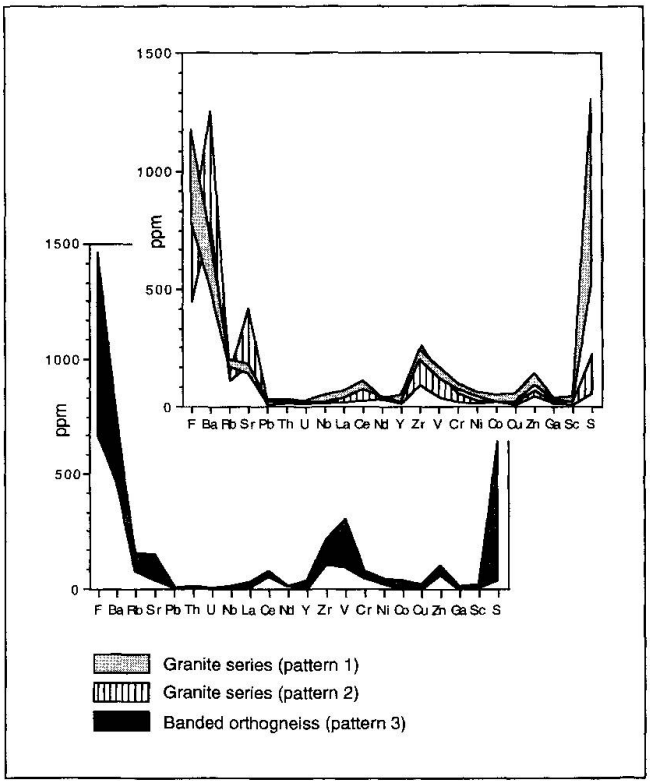

Fig. 7 Diagrams for the minor and trace elements in the banded orthogneiss and in the granite series. Within the granite series, two different minor- and trace element distribution patterns can be distinguished. Pattern 1 displays high F/Ba and F/Rb ratios, high Ba/Rb ratios and low Rb/Sr ratios. Pattern 2 shows F/Ba ratios lower than 1, high Ba/Rb ratios and Rb/Sr ratios lower than 1. The minor and trace element distribution pattern 3 for the banded orthogneiss is similar to pattern 1 of the granite series.

Tab. 2 Bulk chemical composition of I_1 and I_2 rocks from the Bockfjorden area.

The bulk chemical composition was determined by X-ray fluorescence (XRF) analyses with a sequential spectrometer (Philips PW 1404) using natural USGS rock samples for calibration. Rocks were ground in a tungsten carbide mill. Major elements were determined using glass beads which were fused from ignited (at 1050 °C) rocks powders mixed with $Li_2B_4O_7$ in a 1/5 ratio in gold platinum pans at 1150 °C. The intensities were corrected for instrumental drift, background and matrix effects. The trace elements were determined by XRF analyses of 10g rock powder samples using the synthetic background method for which major elements have to be known (NISBET et al., 1979).

	Orthogneiss			Granodiorite							Monzo-granite	Schlieren granite	Aplite	Garnet-bearing aplite		
Sample	B1	B7	B7/1	A7	B10	B11	B12	B13	B17	B21	K9	K13	B9	B16	E4	
Major Elements (wt%)																
SiO_2	68.12	60.44	61.21	65.8	61.33	70.12	61.75	63.57	63.72	60.65	69.15	71.48	75.64	71.3	72.81	
TiO_2	0.75	1.04	1.1	0.75	0.97	0.41	1.03	0.89	0.74	1.02	0.78	0.21	0.05	0.24	0.22	
Al_2O_3	15.25	17.7	17.26	15.5	18.14	16.25	17.62	17.04	16.56	18.8	15.9	15.36	13.93	14.46	14.66	
Fe_2O_3[1]	6.25	8.4	8.98	5.86	8.09	3.89	8.49	7.46	6.89	8.91	5.22	1.54	0.52	1.89	2.5	
MnO	0.04	0.1	0.11	0.09	0.09	0.06	0.1	0.1	0.04	0.08	0.07	0.01	0.01	0.02	0.11	
MgO	1.83	2.51	2.66	1.66	2.38	1.26	2.56	2.26	2.06	2.53	1.7	0.47	0.13	0.51	0.5	
CaO	1.29	1.34	1.26	1.6	1.51	0.82	1.29	1.49	1.74	0.86	2.85	2.18	0.66	1.3	1.33	
Na_2O	1.56	1.92	1.64	1.85	2.1	1.48	1.77	2.3	2.14	1.48	2.78	3.33	2.76	2.19	2.25	
K_2O	3.04	4.45	3.69	3.43	3.65	4.88	3.67	3.45	3.28	4.13	2.42	3.54	5.82	5.84	4.98	
P_2O_5	0.26	0.15	0.09	0.13	0.13	0.12	0.1	0.14	0.07	0.12	0.12	0.05	0.04	0.09	0.11	
Cr_2O_3	0.01	0.01	0.02	0.01	0.01	0	0.02	0.01	0.01	0.02	0	0	0	0	0	
volatiles	1.63	1.5	1.54	1.68	1.52	1.24	1.76	1.43	2.08	2.65	0.66	0.47	0.47	0.6	0.31	
Σ	100.03	99.56	99.56	98.4	99.92	100.53	100.16	100.14	99.33	101.25	100.65	98.64	100.03	98.44	99.78	
Trace Elements (ppm)[2]																detection limit
F	743	1191	1104	816	759	479	1221	886	1179	1129	817	341	327	494	434	50
Ba	570	797	480	726	592	1252	519	570	497	595	1132	817	119	1173	851	10
Rb	119	163	159	155	146	123	166	142	174	194	107	138	257	151	131	3
Sr	121	157	127	178	161	168	127	135	163	123	309	463	45	216	204	3
Pb	< 5	13	< 5	< 5	7	13	10	< 5	< 5	11	< 5	7	11	13	14	5
Nb	< 4	6	6	< 4	10	< 4	9	8	29	9	< 4	< 4	< 4	< 4	< 4	4
La	21	27	26	35	41	< 20	25	39	40	25	41	< 20	< 20	72	35	20
Ce	49	66	63	79	73	17	63	68	84	56	86	< 15	< 15	122	106	15
Nd	< 25	< 25	27	< 25	< 25	< 25	27	< 25	< 25	< 25	< 25	< 25	< 25	41	33	25
Y	27	30	28	27	34	17	35	30	8	33	19	< 3	22	24	33	3
Zr	151	206	226	195	199	82	227	182	199	191	233	91	41	240	241	6
V	99	156	161	99	149	34	153	144	120	135	135	14	< 10	22	24	10
Cr	53	75	81	55	86	21	76	77	70	79	48	< 6	< 6	7	24	6
Ni	29	41	49	24	29	12	42	28	28	44	20	5	< 3	< 3	< 3	3
Co	19	< 4	< 4	16	23	13	< 4	22	21	5	18	7	8	11	6	4
Cu	5	15	27	9	43	< 3	25	21	24	31	< 3	< 3	< 3	< 3	< 3	3
Zn	86	109	115	74	104	45	117	100	121	120	63	18	7	18	12	6
Ga	14	18	19	16	19	9	21	18	20	21	14	15	15	9	8	4
Sc	18	27	28	16	25	8	26	23	10	26	17	2	2	6	9	2
S	134	343	676	< 50	1285	< 50	640	510	903	1192	< 50	< 50	< 50	< 50	137	50

[1] Fe_2O_3 is total iron

[2] Th < 5, U < 10

Tab. 3 Excess of Al_2O_3, trace element patterns (according to Fig. 7) and occurrence of the Al-bearing minerals sillimanite, cordierite and garnet for 15 rock samples from the Bockfjorden area. Crd = cordierite; Grt = Garnet; Sil = sillimanite.
Calculation scheme of Al_2O_3 excess: Rocks were normalized to CIPW norm. As biotite does not occur in CIPW norm, it was calculated according to the reaction orthopyroxene + K-feldspar + corundum –> biotite + quartz. Orthopyroxene was completely consumed, therefore some corundum (expressed as excess Al_2O_3) remained.

Rock type	**Sample**	**Al_2O_3 excess oxide %**	**Trace element pattern** (according to Fig. 7)	**Al - minerals**
Orthogneiss	B1	5.5	3	Crd, Sil
	B7	5	3	Crd, Sil
	B7/1	5.6	3	Crd, Sil
Granodiorite	A7	4.3	1	Crd, Sil
	B10	5.6	1	Crd, Sil
	B11	5.8	2	Crd, Sil
	B12	5.8	1	Crd, Sil
	B13	4,6	1	Crd, Sil
	B17	4.2	1	Crd, Sil
	B21	7.8	1	Crd, Sil
Monzogranite	K9	1.9	2	rare Sil
Schlieren granite	K13	1.6	2	–
Aplite	B9	1.7	–	rare Crd
Grt-bearing aplites	B16	1.8	2	rare Grt
	E4	2.6	2	rare Grt

S-type granitoids (CHAPPELL and WHITE, 1974), indicating that their origin was related to partial melting of crustal rocks.

3) *Is the overall presence of sillimanite and cordierite in the banded orthogneiss, in granodiorite and in aplites and their scarcity or even absence in the monzogranite and in schlieren granite a function of chemical composition?* Table 3 shows that all cordierite- and sillimanite-rich samples from the banded orthogneiss and from the granodiorite display large excess of Al_2O_3. The presence of sillimanite and cordierite has therefore to be considered as a function of bulk rock composition.

4) *Were the rocks with minor Al_2O_3 and the rocks with large excess of Al_2O_3 derived from different protoliths?* Rocks with large excess of Al_2O_3 are generally characterized by the trace element patterns 1 and 3, whereas rocks with low Al_2O_3 display pattern 2 (Tab. 3, Fig. 7). However, sample B11, characterized by trace element pattern 2, displays large excess of Al_2O_3. Therefore, a different origin for high-Al rocks and for low-Al rocks is unlikely.

Magmatic events, structures and metamorphism

Intrusive contacts and their relations to structures and metamorphism were mainly observed on key-outcrops below the tongue of Friedrichbreen (Fig. 5) and on Koveryggen. Observations from these outcrops permit to deduce a detailed sequence of events (Tab. 4, I–IX) for the Bockfjorden area.

I) D_1 DEFORMATION: ISOCLINAL FOLDING OF THE BIOTITE SCHIST

The oldest structure preserved in the studied area is the isoclinal folding F_1 of the banding B_0 in the biotite schist, that is associated to the formation of an axial surface schistosity S_1 (Fig. 8). No F_1 folds have been observed in the marbles. A pre-D_1 set of pegmatite dikes of unknown origin was boudinaged during the D_1 deformation (Fig. 5, loc. 9).

The degree of the accompanying metamorphism is difficult to determine, since these rocks were subsequently affected by the M_2 metamorphism and by a high T-low P metamorphism (VII).

II) I_1: FIRST PHASE OF MAGMATISM; THE INTRUSION OF THE PROTOLITH GRANITOIDS OF THE ORTHOGNEISS

The banded orthogneiss is considered as the granitoid of a first phase of magmatism I_1, that intruded the metasediments after D_1. Evidence for this

Tab. 4 Sequence of events from the Bockfjorden area, compared to the tectonometamorphic evolution of NW Spitsbergen after HJELLE (1979).

	Event	Features	Interpretation	Comparison to Hjelle (1979)
I	**D_1 deformation**	Isoclinal folding of the biotite schist, schistosity S_1 *Amphibolite facies*	a) Early Caledonian phase? b) Grenvillian deformation?	a) F_1: Isoclinal folding, development of cleavage *Upper amphibolite facies*
II	**I_1: First phase of magmatism**	Intrusion of granitoids with a monzogranitic to tonalitic composition, crosscutting D_1 structures Formation of xenoliths of biotite schist and marble	a) Magmatism related to subduction? b) Late Grenvillian intrusions?	
III	**D_2 deformation M_2 metamorphism**	Isoclinal folding F_2 in biotite schist and marble, main schistosity S_2, lineation L_2, shear sense top-to-the N Transformation of the I_1 granitoids to orthogneiss *Amphibolite facies, High T, medium P*	Main Caledonian deformation	F_2: Main recrystallization, isoclinal folding, development of layering and gneissosity *Upper to lower amphibolite facies*
IV	**Migmatite formation**	Segregation of leucocratic layers in the orthogneiss -> banded orthogneiss	Incipient partial melting of the orthogneiss due to crustal extension	F_3: Migmatite formation, emplacement of syntectonic grey granite; weak open folding, initiation of main anticlinorium
V	**D_3 disharmonic folding**	Disharmonic folding F_3	Deformation due to ballooning during the intrusion of I_2?	*Lower amphibolite facies* (Local development of *lowermost granulite facies* east of Smeerenburgfjorden)
VI	**I_2: Second phase of magmatism; the granite series**	Intrusion of granodiorite and monzogranite with aplites and pegmatites, crosscutting biotite schist, marble and I_1 banded orthogneiss Formation of xenoliths of biotite schist, marble and banded orthogneiss *Contact metamorphism*	Emplacement of magmas derived from partial melting of crustal rocks due to extension of the crust	
VII	**High T–low P metamorphism**	Annealing of previous fabrics; formation of cordierite in biotite schist, banded orthogneiss and granodiorite; geotherm of 50°/km *High T, low p metamorphism*	Continuous decompression due to extension of the crust	
VIII	**D_4 deformation**	E-vergent folding F_4, local thrust faults *Upper greenschist facies*	E–W compression, E-vergent thrusting	
IX	**D_5 deformation Bockfjorden antiform**	Open, large scale folding F_5 with subvertical, N–S trending axial surfaces	E–W compression	

sequence is given by enclaves of marble (Fig. 5, loc. 7) and of biotite schist (Fig. 5, loc. 8) that are enclosed by the banded orthogneiss. These enclaves display sharp contacts towards the banded orthogneiss. In addition, they are occasionally rimmed by metamorphic contact zones: The biotite schist enclaves display hornfels rims, whereas wollastonite-bearing mineral assemblages are observed in the marble enclaves. Both, sharp contacts and contact metamorphic rims label them as xenoliths. The isoclinal F_1 folds are documented in the biotite schist xenoliths only, in the banded orthogneiss by contrast, they are not recorded (Fig. 8). This indicates that the biotite schist was intruded by the protolith granitoids of the banded orthogneiss after D_1.

III AND IV) D_2 DEFORMATION, M_2 METAMORPHISM AND MIGMATITE FORMATION

The deformation D_2 is characterized by the isoclinal folding F_2, that is associated to the penetrative schistosity S_2 in the biotite schist and in the marbles. S_2 is the main schistosity in the studied area. The I_1 granitoids were transformed to orthogneiss by D_2 (Fig. 8). In the biotite schist and in the marbles a N–S-trending streching lineation L_2 was formed on the schistosity S_2 (Fig. 2). In the marbles and associated rocks, a strong difference in competence between the metapelitic/metabasic layers and the marble lead to dismembering and to rotation of the metapelitic/metabasic layers during D_2 deformation. Figure 9 shows a dismembered and rotated metapelitic layer. Rotation as well as the asymmetric tails of the boudin point to a simple shear dominant deformation. Some rare asymmetric clasts within the marble indicate a top-to-the N sense of shear. The fold axis of the F_2 isoclinal folds are oriented parallel to L_2. This may be explained by rotation of the fold axis due to strong D_2 simple shearing.

Generally, only relics of the mineral assemblages related to the metamorphism M_2 are preserved except diopside, phlogopite and biotite, that represent the schistosity S_2 in the marbles and in the biotite schist, respectively. This is due to the later high T-low P metamorphism (VII), that lead to an annealing of the fabrics. A biotite schist xenolith displays relics of sillimanite on S_2 that are overprinted by folds of the subsequent deformation D_3 (Fig. 4f). In the orthogneiss oriented sillimanite is included in cordierite and in plagioclase (Fig. 4c). Other inclusions are rounded quarz and biotite (Fig. 4b) as well as rare garnet that are considered to be grown during D_2. The mineral assemblages related to D_2 are summarized in table 1 for all rock types, indicating upper amphibolite facies conditions for M_2.

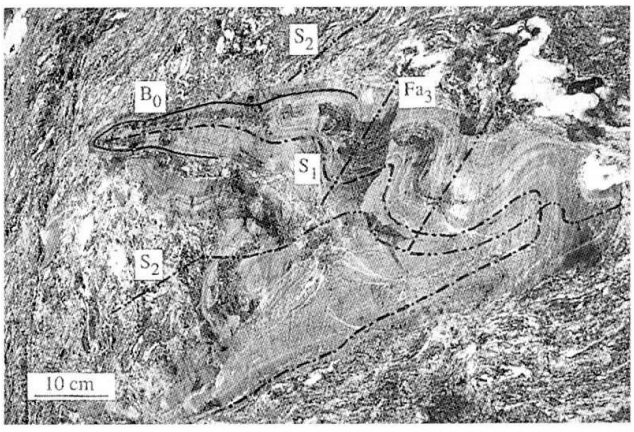

Fig. 8 Xenolith of biotite schist in the banded orthogneiss (see Fig. 5, loc. 8). The xenolith is isoclinally folded by F_2, the axial surface cleavage of which corresponds to the main schistosity S_2 in the orthogneiss. F_2 deforms the axial surface schistosity S_1 in the biotite schist, that is related to the isoclinal fold F_1, affecting the primary banding B_0. The main schistosity S_2 is crenulated by F_3 (Fa_3 = fold axis of F_3) in the orthogneiss and in the biotite schist.

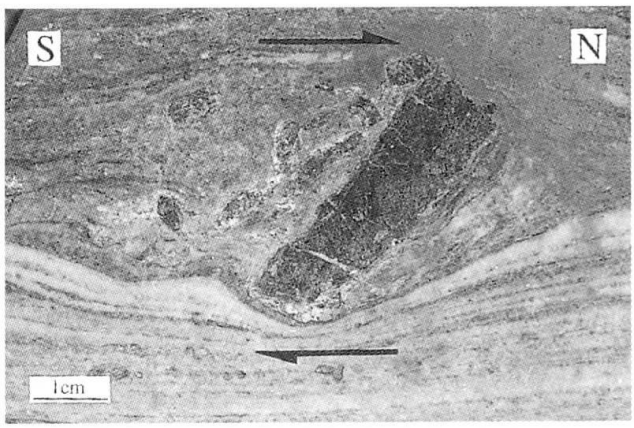

Fig. 9 Rotated boudin of a competent metapelitic layer with asymmetric tails in the marble, indicating a top-to-the N sense of shear.

The banded orthogneiss is characterized by a metamorphic differentiation in melanocratic and leucocratic layers that blurs the schistosity S_2 (Figs 4a, 8, 10). However, leucosomes crosscutting D_2 have not been observed. This feature is interpreted as incipient partial melting of the orthogneiss during late stage- or post-D_2 deformation. The M_2 upper amphibolite facies metamorphism thus reached its thermal peak conditions during late D_2 migmatite formation.

V) D_3 DISHARMONIC FOLDING

Near the contact to the granite series rocks the orthogneiss is overprinted by the disharmonic folding F_3 (Figs 8, 10). Neither F_3 fold axis nor axial surfaces display a systematic orientation. These chaotically oriented structural elements suggest a plastic behavior of the orthogneiss during D_3. The folding F_3 may have occurred during or after migmatite formation. It may be related to a ballooning effect of the granite series intrusion (VI) into the weak migmatites, indicating that the granite series intruded into still hot country rocks.

VI) I_2: SECOND PHASE OF MAGMATISM; THE INTRUSION OF THE GRANITE SERIES

Xenoliths of strongly foliated biotite schist, marble and banded orthogneiss occur in undeformed

Tab. 5 Mineral compositions representative for the M_2 mineral assemblage in orthogneiss (a), for the mineral assemblage of the high P–low P metamorphism in orthogneiss (b) and for the garnet-bearing aplite (c).
Mineral compositions were analyzed using a Cameca SX-50 microprobe, equipped with five crystal spectrometers. Samples were coated with 200 Å of carbon. Operating parameters include an acceleration potential of 15 kV, a beam current of 20 nA and a beam size of 10 Å. Data collection time was 20 s. Natural and synthetic oxides and silicates were used as standards. A ZAF type correction procedure was applied to the data.

	a) Inclusions in cordierite (orthogneiss, sample B1)		b) Equilibrium paragenesis in orthogneiss (sample B1)				c) Garnet-bearing aplite (sample E4)					
weight %	Gar	Bio	Kfs	Plag	Bio	Crd	Gar (core)	Gar (rim)	Bio	Kfs	Plag	av. relative error (2σ) in %
SiO_2	35.8	32.7	64.0	61.0	33.4	46.6	37.5	36.8	34.1	64.5	61.0	1.4 (at 40% level)
TiO_2	< 0.03	4.15	< 0.03	< 0.03	3.46	< 0.03	< 0.03	< 0.03	3.72	< 0.03	< 0.03	3.2 (at 4.0% level)
Al_2O_3	20.7	17.8	19.3	23.8	18.2	31.8	21.7	21.7	19.7	19.0	24.3	1.6 (at 20% level)
Fe_2O_3 [1]	1.93	6.05			1.64		2.38	2.97	3.25		0.12	
FeO	34.5	17.7	< 0.05	< 0.05	20.0	11.2	34.7	32.2	19.6	< 0.05		2.2 (at 20% level)
MnO	4.02	0.10	< 0.03	< 0.03	0.14	0.30	3.18	6.99	0.23	< 0.03	0.07	12.0 (at 0.5% level)
MgO	1.65	6.90	< 0.04	< 0.04	6.79	6.36	3.10	2.18	6.82	< 0.04	< 0.04	1.4 (at 7% level)
CaO	0.81	0.12	0.10	5.50	< 0.02	< 0.02	1.02	0.61	0.04	0.04	5.35	2.4 (at 5% level)
Na_2O	na	0.19	2.04	8.29	0.24	0.35	na	na	0.19	1.59	8.59	10.2 (at 0.2% level)
K_2O	na	8.54	13.8	0.62	9.24	< 0.02	na	na	8.64	14.1	0.39	2.2 (at 9% level)
Cl	na	0.28	na	na	0.30	< 0.02	na	na	0.10	na	na	10.0 (at 0.2% level
H_2O_{calc}		3.77			3.74				3.91			
Σ	99.6	98.5	99.3	99.3	98.1	96.7	103.6	103.4	100.3	99.3	99.8	
Ions calculated on the basis of 8 cations (garnet), 5 cations (feldspars), 3 cations (sillimanite), 18 oxygens (cordierite) and 11 oxygens and cations-Na-K = 7-Ti (biotite)												
Si	2.94	2.56	2.95	2.73	2.63	4.97	2.93	2.90	2.59	2.98	2.71	
Ti	0.00	0.24	0.00	0.00	0.20	0.00	0.00	0.00	0.21	0.00	0.00	
Al	2.01	1.64	1.04	1.26	1.68	3.99	1.99	2.02	1.76	1.04	0.00	
Fe_3	0.12	0.36	0.00	0.00	0.10	0.00	0.14	0.18	0.19	0.00	1.27	
Fe_2	2.37	1.15	0.00	0.00	1.37	1.00	2.27	2.13	1.25	0.00	0.00	
Mn	0.28	0.01	0.00	0.00	0.01	0.03	0.21	0.47	0.01	0.00	0.00	
Mg	0.20	0.80	0.00	0.00	0.80	1.01	0.36	0.26	0.77	0.00	0.00	
Ca	0.07	0.01	0.01	0.26	0.00	0.00	0.09	0.05	0.00	0.00	0.25	
Na	0.00	0.03	0.18	0.72	0.04	0.07	0.00	0.00	0.03	0.14	0.74	
K	0.00	0.85	0.81	0.04	0.93	0.00	0.00	0.00	0.84	0.83	0.02	
Cl	0.00	0.04	0.00	0.00	0.04	0.00	0.00	0.00	0.01	0.00	0.00	
OH	0.00	1.96	0.00	0.00	1.96	0.00	0.00	0.00	1.99	0.00	0.00	

[1] calculated assuming stoichiometry , na: not analysed

or only weakly foliated granodiorite and monzogranite of the granite series (Fig. 5, locs 3, 5 and 6). Figure 5 (loc. 3) and figure 10 show a weakly foliated granodiorite with a xenolith of banded orthogneiss, that displays the schistosity S_2 and disharmonic folds F_3. This demonstrates that D_2 and D_3 occurred prior to the granite series intrusion. Further evidence for this sequence is given by undeformed granodiorite dikes crosscutting the orthogneiss (Fig. 5, loc. 4). The granite series is thus considered to represent the youngest intrusive rocks in the Bockfjorden area.

Marble xenoliths enclosed in granite series rocks (Fig. 5, loc. 5 and loc. 6) display a mineral assemblage that is different from the assemblages observed in the marbles that are not in contact with the granite series intrusion (Tab. 1). This is interpreted as the result of a contact metamorphism in the xenoliths.

VII) HIGH T–LOW P METAMORPHISM

Generally, the high T–low P metamorphism is not associated to deformation. Locally however, it is related to a schistosity at the boundaries of the granite series in the granodiorite and in the monzogranite. As the high T–low P metamorphism annealed the fabrics of all previous events in the metasediments as well as in the banded orthogneiss and in some granite series rocks, it is considered to represent the latest stage of metamorphic crystallization leading to equigranular, polygonal fabrics (Fig. 4a). The schistosity S_2, however, was not blurred by the high T–low P metamorphism, it is preserved either by diopside and phlogopite in the marbles or by biotite in the biotite schist and in the banded orthogneiss.

The high T-low P metamorphism is characterized by the crystallization of cordierite together

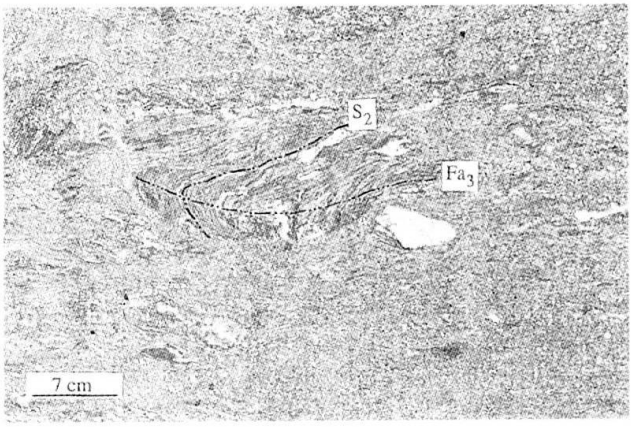

Fig. 10 Granodiorite with xenolith of banded orthogneiss that was folded by F_3 (see Fig. 5, loc. 3). The granodiorite is bare of F_3 folds. S_2 = main schistosity; Fa_3 = fold axis of F_3.

with quartz, plagioclase, K-feldspar and biotite in the biotite schist, in the banded orthogneiss and in the granodiorite of the granite series (Tab. 1, Figs 4a–c). Biotite is intergrown with sillimanite. In K-feldspar and cordierite, rounded biotite and quartz inclusions are common as relics of the M_2 mineral assemblage (Fig. 4b). In the granodiorite M_2-sillimanite and rare garnet are additional inclusions in cordierite. This demonstrates, that cordierite has a metamorphic and not a magmatic origin in the I_2 rocks .

It is noteworthy that the high T–low P metamorphism did not cause crystallisation of cordierite in all rocks of the granite series. Calculated norms based on whole rock chemistry indicate that the occurrence of abundant cordierite is restricted to rocks with a large excess of Al_2O_3 that occurs especially in the granodiorite (Tab. 3). The garnet-bearing schlieren aplites display also excess of Al_2O_3, which is documented by magmatic garnet (Tab. 3, Fig. 4e).

The mineral chemistry of three assemblages, that are representative a) for the M_2 mineral assemblage (relics of garnet, biotite and sillimanite as inclusions in cordierite, sample B1 in Tab. 5), b) for the mineral assemblage of the high T–low P metamorphism in an orthogneiss (sample B1 in Tab. 5) and c) for the garnet-bearing aplite (sample E4 in Tab. 5) corresponds well with analyses from a gneiss-migmatite complex about 45 kms WNW of the studied area (KLAPER, 1986). Klaper calculated temperatures of 650 °C and 0.5–0.6 GPa for the mineral assemblage biotite + cordierite + plagioclase + K-feldspar + garnet + sillimanite + quartz.

As garnet is very rare in the cordierite- and alumosilicate-bearing rocks of the studied area, but biotite, quartz and sillimanite occur frequently as inclusions within cordierite and K-feldspar, the following cordierite forming reaction is proposed for the Bockfjorden area:

biotite + sillimanite + quartz –>
cordierite + K-feldspar + fluid *(1)*

However, biotite and sillimanite included in cordierite are unlikely to represent magmatic minerals. In many peraluminous granites garnet is a primary magmatic phase. The relative scarcity of garnet and the frequent occurrence of sillimanite and biotite might indicate that primary magmatic garnet was decomposed to biotite and sillimanite, according to the reaction:

garnet + K-feldspar + fluid –>
biotite + sillimanite + quartz *(2)*

In the silica undersaturated marble, the mineral assemblage dolomite + calcite + spinel + forsterite (± chlorite) (Tab. 1) is formed by the reaction:

chlorite + dolomite –>
calcite + spinel + forsterite *(3)*

BUCHER-NURMINEN (1981) described this reaction in rocks from a region near the area studied by KLAPER (1986), calculating temperatures of 610–680 °C for assumed pressures of 0.4 GPa.

In the phase diagram of HOLDAWAY (1971) and HOLDAWAY and LEE (1977) (Fig. 11), minimum conditions of 630 °C and 0.3 GPa are indicated for the reaction *biotite + sillimanite + quartz –> K-feldspar + cordierite + fluid* by the absence of

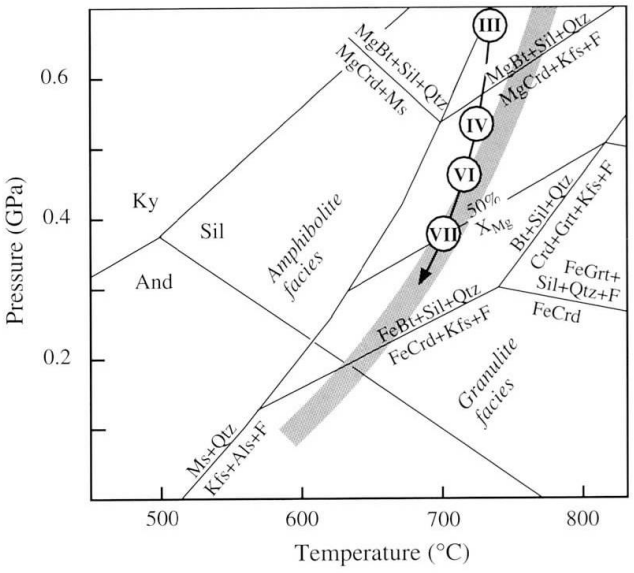

Fig. 11 Phase diagram after HOLDAWAY (1971) and HOLDAWAY and LEE (1977). The roman ciphers refer to the events in table 3: III: Metamorphism M_2, IV: Migmatite formation, VI: Second phase of magmatism I_2, VII: High T–low P metamorphism. Facies boundary (in grey) after SPEAR (1993).

white mica and by the measured X_{Mg} of 0.5 in cordierite. The lack of granulite facies mineral assemblages indicate that the metamorphic conditions did not exceed uppermost amphibolite facies. This is consistent with temperatures of 630–700 °C and pressures of 0.3–0.4 GPa for an X_{Mg} of 0.5 in cordierite. High temperature–low pressure conditions are thus derived for this stage of metamorphism from metapelitic rocks as well as from metacarbonates. On the basis of these data it is suggested that cordierite formed during near isothermal decompression within upper amphibolite facies.

VIII) D_4 DEFORMATION: EAST-VERGENT FOLDING

An east-vergent, open to isoclinal folding F_4 overprints the schistosity S_2, the intensity of which increases to thrust folding on Koveryggen. In isoclinal F_4 fold hinges the mineral assemblage of the high T–low P metamorphism breaks down to an upper greenschist facies mineral assemblage (see Tab. 1; "retrograde metamorphism"). In the marble for example, tremolite crystallizes parallel to the F_4 axial surface, whereas quartz and calcite underwent ductile deformation. This indicates that D_4 postdates the high T–low P metamorphism and therefore also the I_2 intrusion of the granite series.

IX) D_5 DEFORMATION: THE OPEN BOCKFJORDEN ANTIFORM

In the eastern part of the studied area the schistosity S_2 dips to the E and in the western part, it dips to the W (Fig. 2) forming a regional antiform referred to as the Bockfjorden antiform. This antiform structure was described by GJELSVIK (1979). It is, however, not coincident with the east-vergent folding F_4 (Fig. 12): On the eastern side of the Bockfjorden Antiform the F_4 small scale folds are verging towards east. This demonstrates that they cannot be considered as second order folds to the Bockfjorden antiform. In addition, E of Smørstabben the axial surfaces of F_4 folds are overprinted by very open folds of 10 to 500 meters wavelength, that are related to the Bockfjorden antiform. This indicates that the Bockfjorden antiform was formed posterior to D_4.

Discussion

The pre-Devonian basement rocks of the Bockfjorden area were affected by nine tectonothermal events. The features and interpretations of

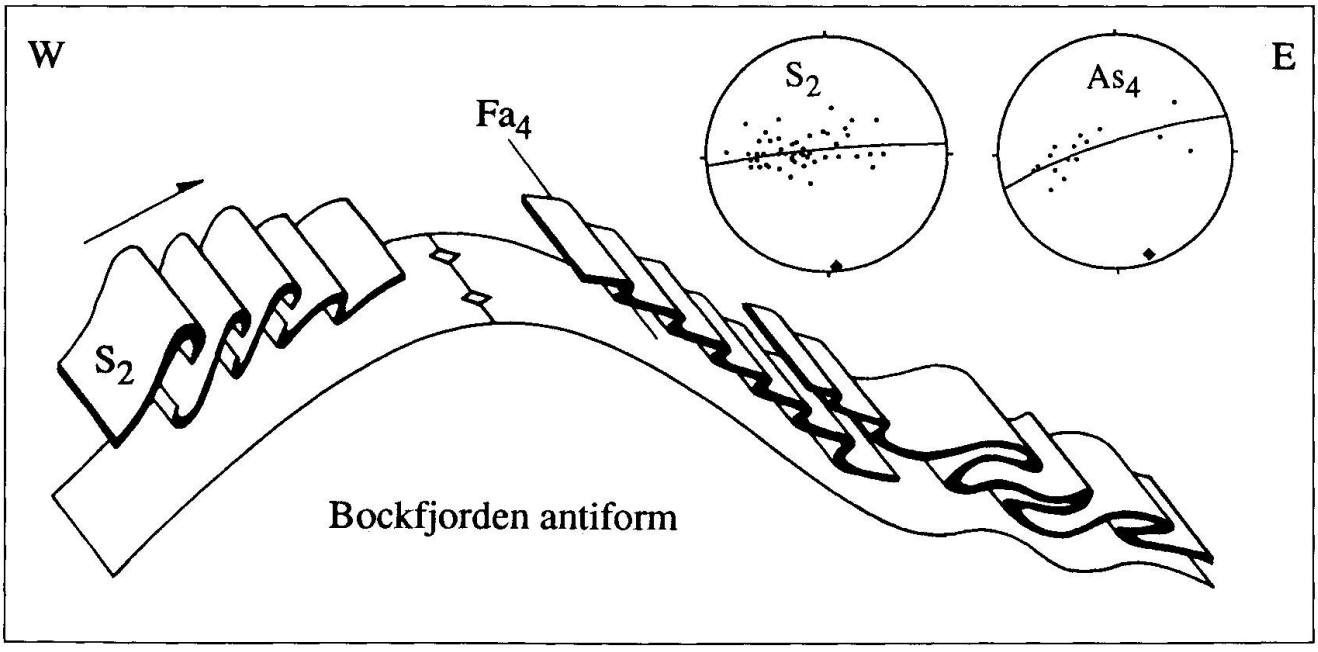

Fig. 12 Schematic structural sketch showing the relation between east-vergent folding F_4 and the Bockfjorden antiform F_5. S_2 = schistosity related to D_2, Fa_4 = fold axis of F_4. As_4 = axial surface of F_4. The sketch is not to scale; the Bockfjorden antiform is about 8 km wide, the small scale folds of F_4 are of a dm scale.
The poles of S_2 as well as of As_4 scatter along a great circle due to subsequent deformation of D_2 and D_4 structures by the F_5 Bockfjorden Antiform. The constructed axis of the Bockfjorden Antiform is subhorizontal and trends approximately in a N–S direction.

this sequence of events are summarized in table 4 (I–IX) and compared with the tectonometamorphic evolution of the basement rocks of central Northwestern Spitsbergen (HJELLE, 1979). According to HARLAND and WRIGHT (1979) central Northwestern Spitsbergen belongs to the same terrane as the Bockfjorden area (Central Terrane). In general, the sequence of events from the investigated area is consistent with the sequence from Central Northwestern Spitsbergen, where three main phases were distinguished (HJELLE, 1979): F_1 (I in Tab. 4), F_2 (III), and F_3 (VI–VII).

The main results are discussed in the light of the subdivision of the Caledonian orogeny into a middle Ordovician period of accretion and subduction and a later middle Silurian continental collision (OHTA et al., 1984; DALLMEYER et al., 1990): First, the main phase of deformation III (D_2) will be treated in relation to the Silurian continental collision. Then, we discuss the significance of the pre D_2 phase II (I_1) and attempt to correlate phase I (D_1) and phase II (I_1) to the regional tectonic evolution. Finally, the phases IV–VII and VIII–IX are discussed.

STRUCTURES RELATED TO COLLISION

The D_2 deformation caused the dominant folding F_2 and foliation S_2 in the Bockfjorden area. It is correlated to the folding F_2 of HJELLE (1979). The related stretching lineation L_2 trends in a N–S direction. Strong stretching and rotation of competent boudins in the marbles (Fig. 9) indicate a simple shear dominated deformation during D_2 with a top-to-the-N sense of shear. The F_2 fold axes are parallel to the stretching lineation. It is suggested that the orientation of the fold axes has been rotated during D_2 shearing. As a consequence, they can not be used to deduce the direction of tectonic transport during D_2. Therefore, D_2 structures are considered to indicate N–S thrusting rather than E–W shortening. However, E–W shortening occurred during the east-vergent folding F_4 and during F_5, causing the general N–S trend of the lithological boundaries in the basement rocks of Northwest Spitzbergen (see Fig. 1).

THE FIRST PHASE OF MAGMATISM I_1: MIGMATITIC FEATURES VERSUS INTRUSIVE RELATIONSHIPS

Enclaves of biotite schist and marble are widespread within the banded orthogneiss. The biotite schist can either be regarded as melanocratic restites or as metasedimentary xenoliths enclosed by magmatic rocks. Sharp contacts towards the banded orthogneiss demonstrate that they were crosscut by the intrusion of the protolith granitoids of the orthogneiss. They must therefore be considered as xenoliths. Evidence for this is also provided by the sequence of tectonometamorphic phases: The xenoliths were enclosed by the protolith granitoids of the banded orthogneiss prior to the deformation D_2, that caused the main schistosity S_2. Migmatite formation by contrast occurred during late stage metamorphism M_2. The xenoliths therefore must not be regarded as restites of the late to post-D_2 migmatite formation. The protolith granitoids of the banded orthogneiss were thus not produced by partial anatexis of the biotite schist. Consequently, we separate the banded orthogneiss from the partly migmatized paraseries of HJELLE (1979) and GJELSVIK (1979) and consider it as an older independent intrusive event.

There is only little evidence for incipient partial melting and migmatite formation during late stage Silurian continental collision. However, as the magmas of the I_2 granite series are inferred to be derived from partial melting of crustal rocks, anatexis must be important in deeper levels of the continental crust at the end of the Caledonian convergence.

SIGNIFICANCE OF THE EVENTS D_1 AND I_1

Intrusive rocks (the first phase of magmatism I_1) predating the middle Silurian collision tectonics D_2 were not yet reported from the Bockfjorden area. They permit more insight into the complex evolution of the pre-Devonian basement rocks; their origin, however, remains unclear.

The deformation D_1 and magmatism I_1 predating the middle Silurian deformation D_2 may be interpreted in two distinct ways. **(a)** They are either related to the middle Ordovician accretion or **(b)** they represent an older event, probably the Grenvillian orogeny.

(a) The isoclinal folding F_1 in the biotite schist points to strong shortening combined with shearing during D_1. It may therefore be explained as a deformation related to early Caledonian accretion. If the biotite schist corresponds to the upper Proterozoic Generalfjella group (GJELSVIK, 1979), it could not have been affected by an orogeny older than the Caledonian one. The I_1 intrusion could then be explained as a magmatism related to early Caledonian subduction. However, the peraluminous composition of the I_1 intrusives and the lack of endogene xenoliths point to partial

melting of the crust. These magmas are thus not expected to be related to accretion and subduction processes.

(b) PEUCAT et al. (1989) describe granitic intrusions of 950–960 Ma from Biskayerhalvøya, the melts of which were at least partially derived from crustal anatexis. If the I_1 intrusives corresponds to these granites, D_1 and I_1 could be related to the Grenvillian orogeny. Then, a correlation of the biotite schist to the Generalfjella group is unlikely and the biotite schist has to be considered as older. Preliminary age determinations on the banded orthogneiss from the Bockfjorden area point to a late Grenvillian age for the I_1 intrusion (OHTA, pers. comm., 1997).

MIGMATITE FORMATION, MAGMA INTRUSION AND HIGH TEMPERATURE – LOW PRESSURE METAMORPHISM DURING CRUSTAL EXTENSION

On the basis of the observations in the Bockfjorden area, the F_3 event of HJELLE (1979) can be subdivided into the four phases IV–VII (Tab. 4). This allows a reconstruction of the late Caledonian high temperature history (Fig. 11).

(IV) The banding of the orthogneiss is interpreted as late D_2 migmatite formation due to incipient partial melting of I_1 granitoid rocks.

(V and VI) The I_2 granite series intrusion crosscuts the partially molten banded orthogneiss. It originated from partial melting of deep seated crustal rocks. Ballooning effects may have caused F_3 disharmonic folding of the late D_2 banding in the orthogneiss. Large volumes of granitic rocks originating from partial melting of crustal rocks are widespread in the Caledonides.

(VII) The formation of cordierite + K-feldspar at the expense of biotite + sillimanite + quartz in all Al-rich rock types including granodiorite of the I_1 granite series during high T–low P metamorphism documents ongoing decompression after the intrusion of the granite series. In the studied area, the high T–low P metamorphism postdates formation of the migmatites, which is in contrast to HJELLE (1979) and KLAPER (1986). Pressure-temperature estimates for the cordierite formation are of 630–700 °C and of 0.3–0.4 GPa, corresponding to uppermost amphibolite facies conditions. The resulting high geotherm of about 50 °C/km is explained with extension of continental crust during high T–low P metamorphism (FOUNTAIN, 1989; HARLEY, 1989). Isothermal decompression (ITD) as it is documented for the Bockfjorden rocks has also been reported from granulite terranes (HARLEY, 1989). Such granulites are interpreted to develop in crust, that was previously thickened by collision. According to Harley, ITD paths are generated during thinning related to rapid tectonic exhumation, that cannot solely be explained by erosion, but must also be related to extension. Thus, the transition from migmatite formation to granite emplacement followed by cordierite formation is interpreted as a post-collisional continuous exhumation of the pre-Devonian basement rocks due to crustal extension.

THE AGE OF LATE-STAGE COMPRESSION

The east-vergent folding F_4 (VIII) developed under retrograde greenschist facies conditions. The Caledonian retrograde metamorphism has been dated to 400–430 Ma by Rb–Sr and Ar–Ar biotite and muscovite cooling ages (DALLMEYER et al., 1990) Therefore, D_4 is considered to be late Caledonian. It is more difficult to constrain the age of the Bockfjorden Antiform (D_5, IX). Large open folds have been mapped in the Devonian sediments east of Liefdefjorden (Figs 1, 2) as well as in Triassic sediments south of the Bockfjorden (HJELLE and LAURITZEN, 1982). Therefore it is likely, that F_5 folding developed during Alpine convergence.

Conclusions

The complex evolution of the basement rocks in the Bockfjorden area permits the distinction of four different periods.

Pre-Silurian evolution: The situation encountered in the Bockfjorden area allows to show that pre-Caledonian igneous rocks form part of the Caledonian basement. These intrusive rocks (I_1) cut an older penetrative deformation (D_1) which is recorded in the biotite schist. This provides evidence for a complex pre-Silurian evolution of the basement rocks, that is probably related to the Grenvillian orogeny.

Caledonian continental collision: The first Caledonian event in this region is recorded by the simple shear dominated deformation D_2, that causes the main schistosity and that leads to N-directed thrusting in the Bockfjorden area. The metamorphic conditions (M_2) reached upper amphibolite facies conditions.

Post-collisional extension: After the pressure peak of M_2 a nearly isothermal decompression under upper amphibolite facies conditions led to migmatite formation in the I_1 intrusive rocks. The subsequent emplacement of I_2 S-type granitoid

melts provides evidence for anatexis in deeper levels of the crust. Ongoing decompression led to a high T–low P metamorphic overprint at conditions of 630–700 °C and 0.3–0.4 GPa, that is characterized by the formation of cordierite + K-feldspar at the expense of sillimanite + biotite + quartz. The evolution from partial melting to granite emplacement followed by high T-low P metamorphism related to a geotherm of about 50 °C/km provides evidence for a continuous exhumation of the crust due to crustal extension subsequent to collision. This may be interpreted as a collapse of the Caledonian thickened crust.

Late stage compression: F_4 folding corresponds to late Caledonian shortening whereas F_5 may have developped during Alpine convergence.

Acknowledgements

We had the opportunity to participate in an expedition of the Swiss Alpine Club in summer of 1992, that visited the Bockfjorden area. Fieldwork was financially supported by the Grubenmann Fonds of the Institut für Mineralogie und Petrographie, ETH Zürich, by a travel grant from Jelmoli Zürich and from Ems Chemie. L.B. was supported by a travel grant from the Martha-Selve-Gertsen-Stiftung. We appreciate the help of Albrecht Steck, Volkmar Trommsdorff and Neil Mancktelow, who commented earlier versions of the manuscript. Fruitful communication with Yoshihide Ohta greatly improved the manuscript. Reviews of Eva M. Klaper and of K. Bucher are greatfully acknowledged.

References

AMUNDSEN, H.E.F. (1987): The lithosphere beneath northwestern Spitsbergen: evidence from upper mantle and lower crustal xenoliths. Ph.D. Thesis, University of Oslo, 128 pp.

BATES, R.L. and JACKSON, J.A. (1987): Glossary of Geology. American Geological Institute, Alexandria, Virginia.

BUCHER-NURMINEN, K. (1981): Petrology of chlorite-spinel marbles from NW-Spitsbergen (Svalbard). Lithos 14, 203–213.

CHAPPELL, B.W. and WHITE, A.J.R. (1974): Two contrasting granite types. Pacific Geology 8, 173–174.

DALLMEYER, R.D., PEUCAT, J.J. and OHTA, Y. (1990): Tectonothermal evolution of contrasting metamorphic complexes in northwest Spitsbergen (Biskayerhalvøya): Evidence from $^{40}Ar/^{39}Ar$ and Rb/Sr mineral ages. Geol. Soc. Am. Bull. 102, 653–663.

FOUNTAIN, D.M. (1989): Growth and modification of lower continental crust in extended terrains: the role of extension and magmatic underplating. In: MEREU, R.F. et al. (eds): Properties and processes of Earth's lower crust. Amer. Geophys. Union monogr. 51, 287–299.

GEE, D.G. and HJELLE, A. (1966): On the crystalline rocks of northwest Spitsbergen. Norsk Polarinstitutt Årbok 1964, 32–45.

GEE, D.G. and MOODY-STUART, M. (1966): The base of the Old Red Sandstone in central north Haakon VII Land, Vestspitsbergen. Norsk Polarinstitutt Årbok 1964, 57–68.

GEE, D.G., SCHOUENBORG, B., PEUCAT, J.J., ABAKUMOV, S.A. KRASIL'SCIKOV, A.A. and TEBENKOV, A. (1992): New evidence of basement in the Svalbard Caledonides: Early Proterozoic zircon ages from Ny Friesland granites. Norsk Geologisk Tidsskrift 72, 181–190.

GEE, D.G., BJÖRKLUND, L. and STØLEN, L.K. (1994): Early Proterozoic basement in Ny Friesland – implications for the Caledonian tectonics of Svalbard. Tectonophysics 231, 171–182.

GJELSVIK, T. (1979): The Hecla Hoek ridge of the Devonian Graben between Liefdefjorden and Holtedahlfønna, Spitsbergen. Norsk Polar Institutt, Skrifter 167, 63–71.

HARLAND, W.B. and WRIGHT, N.J.R. (1979): Alternative hypothesis for the pre-Carboniferous evolution of Svalbard. Norsk Polar Institutt, Skrifter 167, 89–119.

HARLEY, S.L. (1989): The origins of granulites: a metamorphic perspective. Geol. Mag. 126, 215–247

HJELLE, A. (1979): Aspects of the geology of northwestern Spitsbergen. Norsk Polar Institutt, Skrifter 167, 37–62.

HJELLE, A. and OHTA, Y. (eds) (1974): Contributions to the geology of northwestern Spitsbergen. Norsk Polar Institutt, Skrifter 158, 107 pp.

HJELLE, A. and LAURITZEN, Ø. (1982): Geological map of Svalbard 1:500'000, Sheet 3G, Spitsbergen northern part. Norsk Polar Institutt, Skrifter 154c.

HOLDAWAY, M.J. (1971): Stability of andalusite and the aluminium silicate phase diagram. Amer. J. Sci. 271, 97–131.

HOLDAWAY, M.J. and LEE, S.M. (1977): Fe–Mg cordierite stability in high-grade pelitic rocks based on experimental, theoretical, and natural observations. Contrib. Mineral. Petrol. 63, 175–198.

HOLTEDAHL, O. (1914): New features in the geology of northwestern Spitsbergen. Amer. J. Sci. 37.

KLAPER, E.M. (1986): The metamorphic evolution of garnet-cordierite-sillimanite gneisses of NW Spitsbergen (Svalbard). Schweiz. Mineral. Petrogr. Mitt. 66, 295–313.

NISBET, E.G., DIETRICH, V.J. and ESENWEIN, A. (1979): Routine trace element determination in silicate minerals and rocks by X-ray fluorescence. Fortschr. Miner. 57, 264–279.

OHTA, Y. (1992): Recent understanding of the Svalbard basement in the light of new radiometric age determinations. Norsk Geologisk Tidsskrift 72, 1–5.

OHTA, Y. (1994): Caledonian and Precambrian history in Svalbard: a review, and an implication of escape tectonics. Tectonophysics 231, 183–194.

OHTA, Y., HIROI, Y. and HIRAJIMA, T. (1984): Additional evidence of pre-Silurian high-pressure metamorphic rocks in Spitsbergen. Polar Research, N.S. 1, 215–218.

PEUCAT, J.J., OHTA, Y., GEE, D.G. and BERNARD-GRIFFITH, J. (1989): U–Pb, Sr and Nd evidence for Greenvillian and latest Proterozoic tectonothermal activity in the Spitsbergen Caledonides, Arctic Ocean. Lithos 22, 272–285.

PIEPJOHN, K., HARLING, U., KLEE, S., MÖLLER, M. and THIEDIG, F. (1992): Geologische Neukartierung der Germaniahalvøya, Haakon VII Land, NW-Spitzbergen, Svalbard. Stuttgarter Geographische Studien 117, 37–54.

SPEAR, F.S. (1993): Metamorphic phase equilibria and pressure – temperature – time path. Min. Soc. Am. Washington D.C., Monograph Series, 799 pp.

TUCHSCHMID, M. and SPILLMANN, P. (1992): Neogene and Quarternary volcanism on Spitsbergen – the revival of an Arctic Hot Spot. Schweiz. Mineral. Petrogr. Mitt. 251–270.

Received August 25, 1997; revision accepted January 15, 1998.